

Imaging Analysis of Trabecular Bone Texture Based on the Initial Slope of Variogram of Ultra-Distal Radius Digital X-Ray Imaging: Effects on Bone Mineral Density and Age

Jianfeng Chen^{1*}, Qifeng Ying²

¹Department of Radiology and Medical Imaging, Stritch School of Medicine, Loyola University Medical Center, Chicago, USA

²Osteoporosis Center, Zhejiang Provincial People's Hospital, Hangzhou, China
Email: *jfchen@live.com

How to cite this paper: Chen, J.F. and Ying, Q.F. (2022) Imaging Analysis of Trabecular Bone Texture Based on the Initial Slope of Variogram of Ultra-Distal Radius Digital X-Ray Imaging: Effects on Bone Mineral Density and Age. *Open Journal of Radiology*, 12, 78-85.

<https://doi.org/10.4236/ojrad.2022.123009>

Received: June 6, 2022

Accepted: September 6, 2022

Published: September 9, 2022

Copyright © 2022 by author(s) and Scientific Research Publishing Inc. This work is licensed under the Creative Commons Attribution International License (CC BY 4.0).

<http://creativecommons.org/licenses/by/4.0/>



Open Access

Abstract

Background: When applied to trabecular bone X-ray images, a method for analyzing trabecular bone texture based on the initial slope of variogram (ISV) was used to assess the trabecular bone health. **Methodology:** Data from more than two hundred subjects were retrospectively studied. For each subject, a DXA (GE Lunar Prodigy) scan of the forearm was performed, and bone mineral density (BMD) value was measured at the location of ultra-distal radius, X-ray digital image of the same forearm was taken on the same day, and ISV value over the same location of ultra-distal radius was calculated. Pearson's correlation coefficients were calculated to examine the correlation between BMD and ISV of the trabecular bones located at the same ultra-distal radius. ISV values changed with subjects' age were also reported. **Results:** The results show that ISV value was highly correlated with the DXA-measured BMD of the same trabecular bone located at the ultra-distal radius. The correlation coefficient between ISV and BMD with the 95% confident was 0.79 ± 0.09 . They also demonstrated that the age-related changes in trabecular bone health and differentiated age patterns in males and females, respectively. The results showed that the decrease in BMD was accompanied by a decrease in the initial slope of variogram (ISV). **Conclusions:** This study suggests that ISV might be used to quantitatively evaluate trabecular health for osteoporosis and bone disease diagnosis.

Keywords

Trabecular Bone Texture, Digital X-Ray Image, Bone Mineral Density,

1. Introduction

Osteoporosis is a bone disease characterized by low bone mineral density (BMD) and micro-architectural deterioration of bone tissue [1]. The BMD measurement by using dual energy X-ray absorptiometry (DXA) is defined by the World Health Organization (WHO) Working Group as the gold standard and is clinically used to diagnose osteoporosis. BMD is clearly one of the major determinants of bone strength and fracture risk [2] [3] [4], but the assessment of fracture risk by BMD sometime may still lack enough sensitivity [5]. It is clear that other factors in addition to BMD may account for bone strength and fracture risk. They could include bone micro-architecture, bone geometry, and other extra-skeletal factors [5]. The trabecular structure with specific reference to bone micro-architecture, known to affect bone fragility, may not be completely accounted for by standard DXA measurements, but alternative approaches, such as Trabecular Bone Score (TBS), have been proposed in order to overcome this limitation [6] [7]. TBS is defined as the initial slope of the variogram of lumbar spine DXA image, and is a novel texture parameter that evaluates pixel gray-level local variations in a DXA lumbar spine or human femur image and may directly related to bone micro-architecture and fragility fracture risk [6], and might improve the prediction accuracy for major osteoporotic fractures in elderly people [7]. Conceptually, a dense trabecular network, associated with strong mechanical bone strength, produces a projection image with many fine gray-level texture variations of small amplitude and therefore a steep slope of variogram. In contrast, a loose trabecular network, associated with weak mechanical bone strength, produces a projection image with fewer fine gray-level texture variations of large amplitude and therefore a shallow slope of variogram.

Variogram along the direction of perpendicular to radius, $\gamma(\Delta x)$, which is widely used in geostatistical applications, is defined as the expected squared difference between any paired data values $I(x, y)$ and $I(x + \Delta x, y)$ on a trabecular bone image

$$\gamma(\Delta x) = E \left\{ \left[I(x + \Delta x, y) - I(x, y) \right]^2 \right\} \quad (1)$$

and its' initial slope of variogram (ISV) is given by

$$\gamma'(\Delta x) = \frac{E \left\{ \left[I(x + \Delta x, y) - I(x, y) \right]^2 \right\}}{\Delta x} \quad (2)$$

where $I(x, y)$ is the signal at the location of (x, y) within a trabecular bone area and is a random function associated with the trabecular bone network structure varied continuously in space, both (x, y) and $(x + \Delta x, y)$ are the spatial coordinates of locations within trabecular bone, Δx is a lag between

these two separate locations (x, y) and $(x + \Delta x, y)$. $E\{X\}$ is a spatial expectation. This directional variogram only depends on the spatial separation lag Δx , since this gives an intuitive interpretation for the variations of the data in a second-order stationary process.

2. Materials and Methods

2.1. Study Subjects

In order to assess whether the initial slope of variogram (ISV) of digital X-ray images over trabecular bone area located at ultra-distal radius could discriminate subject's bone health, which was defined by BMD values, both radiographic and BMD data from a group of 98 male and 130 female adults, who were recruited and participated in the project of BMD measurements and osteoporosis assessments with radiographer at two hospitals in China, were studied retrospectively. The participants were originally screened by detailed questionnaire, disease history, and physical examination. Their ages ranged from 23 to 87 years old, with an average age of 62 years. Participants were excluded if they had a history of forearm trauma and cancer.

A typical digital X-ray image of the ultra-distal radius, as shown in **Figure 1**, was obtained by using a commercial available digital radiographic system. These digital X-ray images could qualitatively show the image texture difference between normal and abnormal bones due to deteriorate microarchitecture of bone. The acquisition parameters for these digital X-ray images were set as 55 kVp and 10 mAs (100 mA and 100 msec) with a specific SID (source-to-image distance) of 100 cm, and a X-ray focal spot of 0.6 mm. No any added X-ray filtration was used. The digital image detector has $3\text{ k} \times 3\text{ k}$ pixels matrix with a pixel size of 0.139 mm, and the image signal has a gray level depth of 12 bits. In order to reduce Heel effect of X-ray imaging, the region of interest (ROI) was put in the center of X-ray beam (around the original point of X-ray image).



Figure 1. Representative image depicting the ultra-distal radius of subjects obtained using a digital X-ray imaging system.

2.2. Calculation of the Initial Slope of the Variogram

In our study, the logarithm of digital image signal, $\ln[I(x, y)]$, was used, since the physical dimension of bone in X-ray projection direction, $Z(x, y)$, verses the image signal, $I(x, y)$, has the following logarithm relationship:

$$Z(x, y) = \ln \left[\frac{I_0}{I(x, y)} \right] / \mu, \text{ where } \mu \text{ is the effective attenuation coefficient of}$$

trabecular bone, both I_0 and $I(x, y)$ are the image signals before and after X-ray went through a specific bone material with the thickness of $Z(x, y)$. The initial slope of variogram (ISV) of digital X-ray image signal, $\ln[I(x, y)]$, from the region of interest (ROI) of ultra-distal radius area was computed as the mean of variance values at different locations that have the same value of lag Δx :

$$\gamma'(\Delta x) = \frac{1}{2M\Delta x} \sum_{i=1}^M \sum_{j=1}^N \left\{ \ln[I(x_i, y_j)] - \ln[I(x_i + \Delta x, y_j)] \right\}^2 \quad (3)$$

where $M \times N$ is the total number of data pairs $\ln[I(x_i, y_j)]$ and $\ln[I(x_i + \Delta x, y_j)]$ within the region of interest (ROI). ROI starts at the bifurcation of the radius and ulna, and the coverage range is 1/12 length of radius as shown in **Figure 2(a)**, and is similar to the ROI of ultra-distal radius defined for GE Prodigy, and has an enclosed area within ultra-distal radius [8], as shown in **Figure 2(b)**. Δx is a lag distance between two separate locations (x_i, y_j) and $(x_i + \Delta x, y_j)$, and is set as two pixels size, 0.28 mm, in our computation.

2.3. BMD Measurements with DXA

The measurement of BMD at ultra-distal radius was performed for all participants using a GE Lunar Prodigy DXA scanner (GE Healthcare, Madison, WI) running enCORE software version 13.31, which is designed to make DXA even more powerful. During the study, the DXA scanner was calibrated with a GE

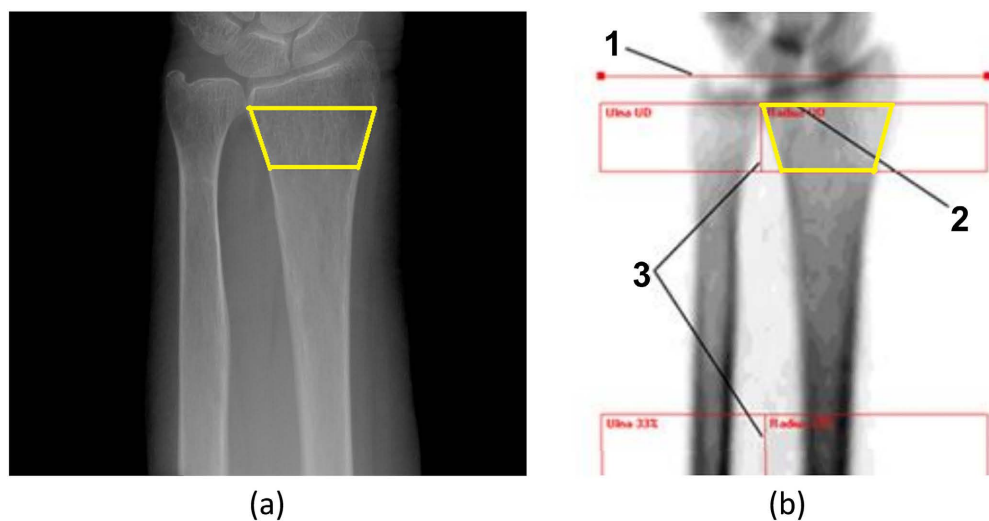


Figure 2. ROI used for our analysis starts from the reference point of the bifurcation of the radius and ulna, and the coverage range is 1/12 length of radius as shown in (a), and is similar to the ROI of ultra-distal radius area defined for GE Prodigy as shown in (b) [8].

Lunar aluminum spine phantom to avoid any affect from significant drift and/or shift on our study. For BMD measurements, each subject was asked to sit beside the scanning table in a chair without any arms or wheels. The subject was asked to keep the forearm immobile during scanning and the forearm was scanned parallel to the long axis of the table. The scanning range was from the center of wrist to the proximal forearm according to the operation manual provided by the manufacturer.

2.4. Statistical Analysis

ISV as the functions of BMD, ages, and BMI for both men and women were analyzed. Pearson correlation coefficients for ISV and BMD of trabecular bone located at ultra-distal radius were calculated [9]. Person correlation coefficient is given by

$$R = \frac{\sum_{i=1}^{N_1} (X_i - \bar{X})(Y_i - \bar{Y})}{\sqrt{\sum_{i=1}^{N_1} (X_i - \bar{X})^2 \sum_{i=1}^{N_1} (Y_i - \bar{Y})^2}} \quad (4)$$

where R is the Pearson correlation coefficient, X_i is the ISV value shown in Equation (3), and Y_i is the BMD value for the for the patient i . \bar{X} is the mean of X_i , \bar{Y} is the mean of Y_i , and N_1 is the total of patients. Then, both linear regressions and their R-squared values are also calculated. Here R-squared values show how well the data fit the regression model.

3. Results

Participant Characteristics

Among 228 subjects, 43% were men (98/228) with an average age 57.7 ± 19.5 years, and 57% were women (130/228) with an average age 65.3 ± 13.3 years. The BMD of ultra-distal radius was 0.522 ± 0.088 g/cm² for men, and 0.350 ± 0.103 g/cm² for women. The average ISV of ultra-distal radius was 0.481 ± 0.092 cm⁻¹ for men, and 0.322 ± 0.075 cm⁻¹ for women. The Pearson correlation coefficient between BMD and ISV for the trabecular bone located at ultra-distal radius with 95% confident is 0.79 ± 0.08 , and R squared value is 0.56, as shown in **Figure 3**. ISV as the function of subject's age was shown in **Figure 4**. These results show that ISV was slightly negatively correlated with subject's age. R squared values between ISV and subject's age were 0.0478 for men and 0.300 for women.

4. Discussion

Osteoporosis is defined as a systemic skeletal disease characterized by low bone mass density and micro-architectural degradation of bone tissue, with an increase in bone fragility to fracture. Current study shows that a decrease in BMD could often be accompanied by bone micro-architectural deterioration. Po-thuau *et al.* introduced a parameter called trabecular bone score (TBS) which is a texture index that evaluates pixel gray-level variations of 2D projection images of the trabecular bone from human lumbar spines acquired by DXA scanners

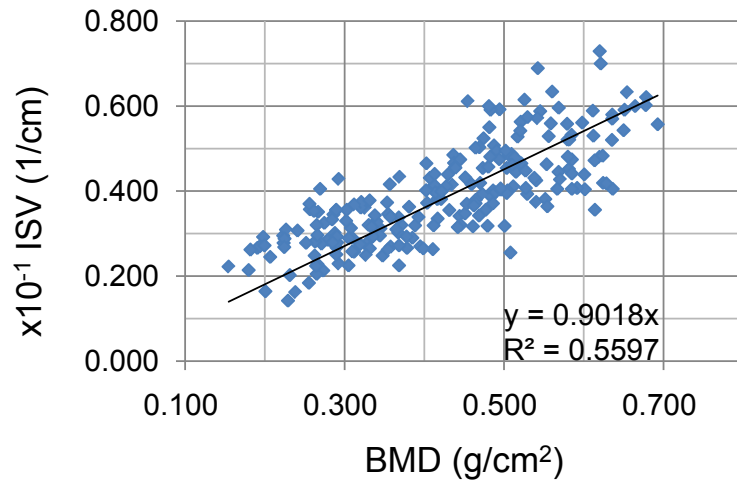
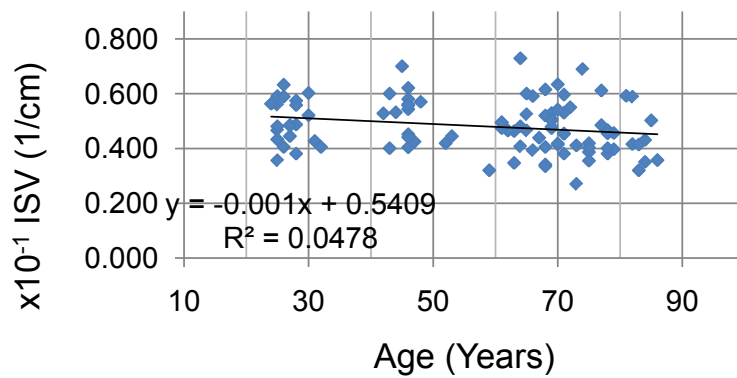
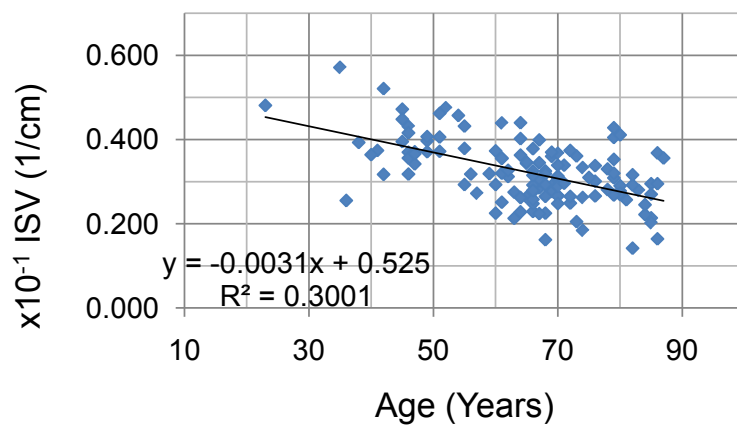


Figure 3. The correlation coefficients between BMD and ISV of trabecular bone located at ultra-distal radius, and linear regression line with R-squared value = 0.5597, is given here.



(a)



(b)

Figure 4. The results of ISV of trabecular bone located at ultra-distal radius as a function of subjects' age for men (a) and women (b). ISV is less sensitive to subject's age for men compared with women.

[5], providing an indirect index of trabecular architecture. TBS is defined as the initial slope of the log-log transform of variogram [10], which describes the rate

of changes of variance with respect to a lag distance. Significant correlations were observed between TBS and microarchitecture parameters (e.g. bone volume fraction and trabecular number) of trabecular bone from human femurs and lumbar spines [5]. A dense trabecular structure produces a 2D image with a large number of pixel value variations of small amplitude, and consequently a steep slope at the origin of the variogram and a high TBS value. Conversely, a 2D projection of deteriorated bone architecture produces an image with a low number of pixel value variations of high amplitude, and therefore a mild slope at the origin of the variogram and a low TBS. It was found that TBS correlated positively with the BMD and decreased with age [11]. Our results were in agreement with the results of these previous studies.

The results of current studies show that ISV might potentially be quantitatively used to assess age-related and/or pathological changes in the microstructures of ultra-distal radius, which could effect on bone fragility. If the ISV proposed in this study was applied, a quantitative measurement could be made directly on the plain projection X-ray image obtained from routine clinical practice. In addition to quantify the microstructures of ultra-distal radius as shown in current study, the ISV may also be used to quantitatively assess the microstructures of other trabecular bones. The overall purpose of such investigations will be to see whether radiographically determined trabecular micro-architecture bone can improve a clinician's capability to estimate patients' risk of osteoporotic fracture, over that obtainable by using bone mass measurements alone.

5. Limitations

There are several limitations for this study. First, the isotropic randomness of trabecular bone microstructure was assumed in current study, the bone micro-structures at ultra-distal radius might not be ideally isotropic, and the irregular shape of the trabecular bone located at ultra-distal radius could create a non-uniform bone image due to the variety of bone thickness along the projection direction in clinical setting. Second, all measures reported for BMD in this study were obtained from a GE Lunar Prodigy DXA scanner and therefore our findings may not necessarily be extrapolated to scanners from other manufacturers, as the ROI at ultra-distal radius site could be slightly different for different DXA scanners. Third, a standardized setting of X-ray image acquisition procedures needs to be developed, since the image signal received by X-ray detector depends on both the energy and intensity of X-ray. This should include the development of automatic compensation techniques related to digital detector's properties, as well as methods to generate good reproducibility. In current study, we only analyzed the images of trabecular bone, didn't address any images of cortical bone.

6. Conclusion

The results of this study demonstrate that the ISV measured from high resolu-

tion digital X-ray image of the distal radius is highly correlated with the BMD measurements of the ultra-distal radius using DXA. The imaging analysis of trabecular bone texture may potentially play an alternative role in the study of osteoporosis and bone health.

Conflicts of Interest

The authors declare no conflicts of interest regarding the publication of this paper.

References

- [1] WHO Study Group (1994) Assessment of Fracture Risk and Its Application to Screening for Postmenopausal Osteoporosis. World Health Organization Technical Report Series, Geneva.
- [2] Lin, J., Boechat, M.I., Deville, J.G., Gilsanz, D., Stiehm, R., Gilsanz, V., Salusky, I. and Nielsen-Saines, K. (2012) Quantitative Computerized Tomography (QCT) versus Dual X-Ray Absorptiometry (DXA) in the Assessment of Bone Mineral Density of HIV-1 Infected Children. *World Journal of AIDS*, **2**, 306-311. <https://doi.org/10.4236/wja.2012.24041>
- [3] Stone, K., Seeley, D., Lui, L., Cauley, J., Ensrud, K., Browner, W., Nevitt, M. and Cummings, S. (2003) BMD at Multiple Sites and Risk of Fracture of Multiple Types: Long-Term Results from the Study of Osteoporotic Fractures. *Journal of Bone Mineral Research*, **18**, 1947-1954. <https://doi.org/10.1359/jbmr.2003.18.11.1947>
- [4] Rice, J.C., Cowin, S.C. and Bowman, J.A. (2003) On the Dependence of the Elasticity and Strength of Cancellous Bone on Apparent Density. *Journal of Biomechanics*, **21**, 155-168. [https://doi.org/10.1016/0021-9290\(88\)90008-5](https://doi.org/10.1016/0021-9290(88)90008-5)
- [5] Pothuau, L., Carceller, P. and Hans, D. (2007) Correlations between Grey-Level Variations in 2D Projection Images (TBS) and 3D Microarchitecture: Applications in the Study of Human Trabecular Bone Microarchitecture. *Bone*, **42**, 775-787. <https://doi.org/10.1016/j.bone.2007.11.018>
- [6] Krueger, D., Fidler, E., Libber, J., Berengere, A., Hans, D. and Binkley, N. (2014) Spine Trabecular Bone Score Subsequent to Bone Mineral Density Improves Fracture Discrimination in Women. *Journal of Clinical Densitom*, **17**, 60-65. <https://doi.org/10.1016/j.jocd.2013.05.001>
- [7] Iki, M., Fujita, Y., Tamaki, J., Kouda, K., Yura, A., Sato, Y., Moon, J., Winzenrieth, R., Okamoto, N. and Kurumatani, N. (2015) Trabecular Bone Score May Improve FRAX1 Prediction Accuracy for Major Osteoporotic Fractures in Elderly Japanese Men: The Fujiwara-Kyo Osteoporosis Risk in Men (FORMEN) Cohort Study. *Osteoporosis International*, **26**, 1841-1848. <https://doi.org/10.1007/s00198-015-3092-3>
- [8] Healthcare, G.E. (2010) Lunar enCORE-Based X-Ray Bone Densitometer User Manual.
- [9] Mukaka, M.M. and Corner, S. (2012) A Guide to Appropriate Use of Correlation Coefficient in Medical Research. *Malawi Medical Journal*, **24**, 69-71.
- [10] Pothuau, L. (2009) Method for Determining a Three-Dimensional Structure from a Two-Dimensional Image, in Particular a Bone Structure. United States Patent, US7609867B2.
- [11] Cheng, P., Qi, H., Di, W., Liu, J., Yu, J., Lv, S., Shen, Y., Zha, J., Cai, J., Lai, B. and Ding, G. (2016) Establishment of TBS Reference Plots and Correlation between TBS and BMD in Health Mainland Chinese Women. *Archives of Osteoporosis*, **11**, Article No. 5. <https://doi.org/10.1007/s11657-015-0254-z>